

Self-Calibration of a Leica HDS7000 Scanner

Khalil AL-MANASIR, China and Derek D LICHTI, Canada

Keywords: Terrestrial Laser Scanning, Self-Calibration, Systematic Errors.

SUMMARY

Terrestrial laser scanners are widely used for metric applications of 3D modelling of buildings, bridges, tunnels and other structures. In common with any measurement system, the calibration of the laser scanner is of paramount importance to achieve the maximum possible accuracy. Even if a calibration certificate of the scanner is provided by the vendor, the scanner should be checked from time to time for any systematic errors using special equipment and facilitates. This process is time consuming as the scanner needs to be sent to vendor for long time. The self-calibration method provides a very flexible yet rigorous solution that allows scanner users to calibrate instruments themselves. This paper uses the self-calibration approach to develop and establish a calibration model for Leica HDS7000 phase-based terrestrial laser scanner. The calibration process and a calibration field of signalised targets designed to perform the calibration are described. The final results show the importance and potential of the self-calibration method, especially when high-precision measurements are required. Two highly-redundant (nearly 5000 degrees-of-freedom) calibrations of the scanner were conducted on separate dates. Statistically significant angular errors (collimation axis, trunnion axis; vertical axis-horizontal encoder non-orthogonality and vertical circle index) were found in both datasets. A small (0.6 mm), but statistically significant, rangefinder offset parameter was also estimated. The improvements gained as a result of the modelling were 41% and 45% in the horizontal angle direction residuals and 54% and 87% in the elevation angle residuals for the first and second datasets, respectively.

Self-Calibration of a Leica HDS7000 Scanner

Khalil AL-MANASIR, China and Derek D LICHTI, Canada

1. INTRODUCTION

The terrestrial laser scanner (TLS) is a line-of-sight instrument that can directly acquire dense 3D point clouds in a very short time. Recent advances in the terrestrial laser scanner design has expanded the consumer and research market in surveying, mapping, civil, and other engineering applications. The accuracy of the scanner is limited by the systematic instrumental errors, which means that it has to be properly calibrated to ensure that the terrestrial laser scanner is performing at its optimal condition. Laser scanner calibration is performed to identify the systematic errors (calibration parameters) in the instrument. These parameters together constitute a calibration model, which can be used to correct the systematic instrumental errors. Therefore, it is possible to improve the accuracy in the software instead of disassembling the instrument for re-calibration. Unlike traditional geodetic and photogrammetric instruments, the single point measurement accuracy of modern terrestrial laser scanners is limited due to the use of reflectorless electronic distance measurements (EDM) and the observation of both the horizontal and vertical circle readings on only a single face. In this paper, the self-calibration is used for the determination of all systematic errors of a terrestrial laser scanner simultaneously with all other system parameters based on optimizing the instrument's raw measurements. Therefore the single point accuracy of the laser scanner is improved and not just the noise in geometrical form fitting.

Systematic errors can exist in modern terrestrial laser scanners even after the manufacturer's precise laboratory calibration. Numerous researchers around the world have independently identified systematic trends in the laser scanner's residuals that deteriorate the range and angular measurement precision and accuracy of the laser scanner (Lichti et al., 2000, 2002; Böhler et al., 2003; Kersten et al., 2004, 2005; Amiri Parian and Grün, 2005; and Molnár et al., 2009). To recover the laser scanner's true performance, different calibration schemes have been developed over the years. They can be broadly classified as point based approach (Lichti, 2007; Reshetyuk, 2006, 2009; Schneider and Schwalbe, 2008) or feature based (e.g. planes, cylinders or other object) approach (Gielsdorf et al., 2004; Dorninger et al., 2008; Chow et al., 2013; Kuhlmann and Holst, 2014; Chan et al., 2015). Both methods rely on capturing a large redundant set of observations with a laser scanner from different position and orientations. The main benefit of this calibration approach is that no specialized equipment (e.g. EDM baselines and oscilloscope) is required and a user can frequently identify, model, and update the sensor's systematic errors in both pulse-based and phase-based TLS systems without disassembling the instrument.

This paper reports an investigation into the systematic error modelling and self-calibration of the Lecia HDS7000 scanner with the aim of improving the accuracy of collected point clouds. The motivation was systematic errors that could be observed in point clouds acquired with this instrument. An example exhibiting a discontinuity of several centimetres (1.9 cm) at 5m from the scanner is shown in Figure 1.

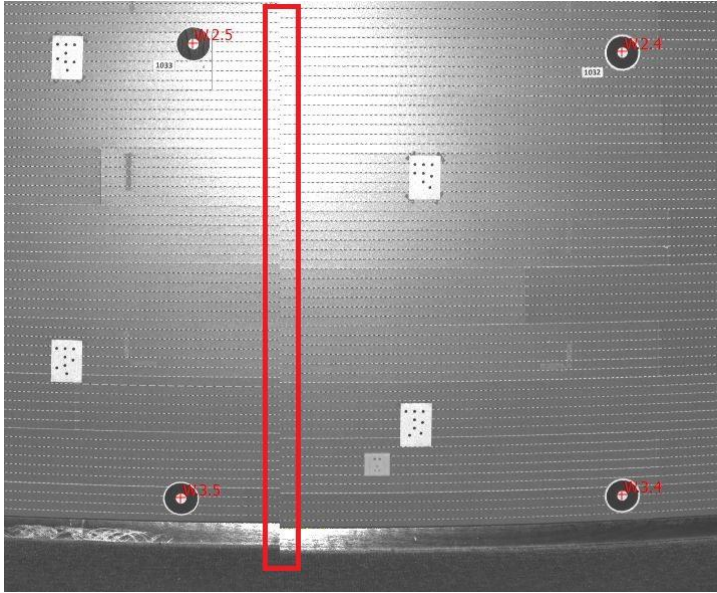


Figure 1. HDS7000 intensity image showing the discontinuity in data acquired over an indoor 3D target field.

2. TLS SELF-CALIBRATION

2.1 Observation Equations

The geometric model of calibration is based on the assumption that the instrumental errors of a typical laser scanner corresponds to those of a total station. The raw TLS measurements are made in a spherical coordinate system. Modern TLS systems operate very much like a total station with additional scanning mechanisms. They measure the range, ρ , horizontal direction, θ , and vertical direction, α , to a single point. Such similarities in instrumentation makes it logical to base the systematic error modelling of TLS systems on total stations, which have been widely explored (Rüeger, 1992; Wolf and Ghilani, 2006). The geometric calibration of each and every point i in scanner space j is carried out following Equation 1.

$$\rho_{ij} = \sqrt{x_{ij}^2 + y_{ij}^2 + z_{ij}^2} + \Delta\rho$$

$$\theta_{ij} = \tan^{-1}\left(\frac{x_{ij}}{-y_{ij}}\right) + \Delta\theta \quad (1)$$

$$\alpha_{ij} = \tan^{-1} \left(\frac{z_{ij}}{\sqrt{x_{ij}^2 + y_{ij}^2}} \right) + \Delta\alpha$$

where ρ_{ij} , θ_{ij} , α_{ij} are the range, horizontal circle reading, and vertical circle reading, respectively, of point i from scan station j ; x_{ij} , y_{ij} , z_{ij} are the Cartesian coordinates of point i at scan station j ; and $\Delta\rho$, $\Delta\theta$, and $\Delta\alpha$ are the additional systematic correction terms for range, horizontal direction, and vertical angle, respectively.

The transformation parameters between the Cartesian object space and scanner space systems can be expressed as a 3D rigid body transformation:

$$\begin{pmatrix} x_{ij} \\ y_{ij} \\ z_{ij} \end{pmatrix} = M_j \left[\begin{pmatrix} X_i \\ Y_i \\ Z_i \end{pmatrix} - \begin{pmatrix} X_{oj} \\ Y_{oj} \\ Z_{oj} \end{pmatrix} \right] \quad (2)$$

The rotation matrix M is formed from three sequential rotation angles, ω_j , ϕ_j and κ_j . The position of the scanner j in object space reference frame is expressed by the translations X_{oj} , Y_{oj} and Z_{oj} . The object space coordinates of point i are expressed by X_i , Y_i and Z_i . Once the six transformation parameters between the scanner point cloud and the object space are computed, the XYZ coordinates of all scan points can be transformed into the object space coordinate system.

2.2 Systematic Error Models

Though general models for the systematic errors in TLS instruments have been published (e.g. Lichti, 2007), the actual set of additional parameters (APs) required for a given instrument cannot necessarily be determined *a priori*. Though prior knowledge of an instrument can guide model choice, one must find an optimal trade-off between goodness-of-fit and allowable bias. While on the one hand the error model should model all systematic effects, the number of APs should be kept as low as possible to avoid over-parameterization. Graphical and statistical analyses can guide the decision, which can be automated (e.g., García-San-Miguel and Lerma, 2014).

For the scanner studied in this investigation, a Leica HDS7000, the following error systematic model was identified. Examples of some of the errors are provided in Section 4.

$$\Delta\rho = a_0$$

$$\Delta\theta = b_1 \sec(\alpha_{ij}) + b_2 \tan(\alpha_{ij}) + b_3 \sin(\theta_{ij}) + b_4 \cos(\theta_{ij}) \quad (3)$$

$$\Delta\alpha = c_0$$

where a_0 is the rangefinder offset; b_1 is the collimation axis error; b_2 is the trunnion axis error; b_3 and b_4 are the coefficients of the non-orthogonality between the horizontal angle encoder plane and the vertical axis; and c_0 is the vertical circle index error.

2.3 Network Design and Additional Observations

To minimize the correlation between the calibration parameters (e.g. vertical circle index error and the tilt angles ω and ϕ), proper network design has been considered. Network design measures include acquisition of scan data from multiple locations and orientations within a large room comprising many target primitives. A large variety of range observations and collection of angular data over the full range is also suggested. Additional condition equations can be included in the least squares adjustment. For example, to mathematically describe the fact that the scanner was levelled during the scanning process, Equation 4 can be adopted for each scan location.

$$\begin{aligned}\omega_j &= 0 \\ \phi_j &= 0\end{aligned}\tag{4}$$

3. EXPERIMENT DESCRIPTION

For the determination of calibration parameters a test field at Nottingham University Ningbo, China was constructed in a 17m x 10m x 3m room. Despite the fact that the maximum measured distances were relatively short, the data acquisition was performed indoors in a room where the temperature, pressure, and humidity were homogeneous and controlled in order to minimize the effects of horizontal and vertical refraction. The 260 planar calibration targets are distributed throughout the room in order to completely fill the scanner's field-of-view. The chosen target design has a black background printed onto a circular paper with 5.5 cm in radius using a LaserJet printer. The central white circle has a radius of radius of 1.8 cm.

The Leica HDS7000 scanner was set up on a special wooden surveying tripod, tribrach, and spider combination, and securely taped to the floor during data acquisition (Figure 2). The dual axis compensation of the scanner was activated in order to precisely level the instrument. The point density of all the scans was set to 1.1 mm at a 1 m distance and due to time limitations only a single distance measurement was made to each point.



Figure 2. Scanner set up for data acquisition.

Eight scans were captured from two nominal scan locations chosen to maximize the baseline distance. At each location, four leveled scans were captured, each having a heading (κ angle) that differed by approximately 90° . Data were acquired from ranges of 1.4 m to 11.9 m, throughout the scanner's full 180° horizontal field-of-view and through a 300° vertical field-of-view. The same data acquisition procedure was followed on two separate dates.

The centroid of each planar target was measured based on the intensity difference and least squares geometric form fitting as explained in Chow et al. (2010). For each of the two datasets, the centroids of these targets captured in each scan were then related to other scans in network based on the mathematical models presented in Section 2 with the datum defined via inner constraints on object points. In addition to the spherical coordinate observations, the levelled-instrument conditions scans were also included in the least squares, self-calibrating bundle adjustment. The 3D object space coordinates of each target, the APs of the scanner's systematic error model, and the exterior orientation parameters of each scan station (ω_j , ϕ_j , κ_j , X_{O_j} , Y_{O_j} and Z_{O_j}) were solved simultaneously. The observations were weighted according to four groups (ρ , α , θ and tilt angles). All observations within a group were assumed to be of equal precision with the exception of ranges, for which the following incidence angle (β) dependent model (Soudarissanane et al., 2011) was used

$$\sigma_\rho = \sigma_\perp \sec(\beta_{ij}) \quad (5)$$

where σ_\perp is the range precision at normal incidence. The relative weights of each group were tuned with iterative variance component estimation.

4. RESULTS AND ANALYSES

Table 1 summarizes the self-calibration adjustment metadata for both datasets. As can be seen, both were highly-redundant networks with nearly 5000 degrees-of-freedom. Table 2 quantifies the improvement gained as a result of adding the six aforementioned APs to the models. Clearly there is significant improvement in the angular quantities with improvements of 41% to 87% and, in both datasets, the final angular precision is about at the 10".

Table 1. Self-calibration adjustment metadata.

	Dataset 1	Dataset 2
Number of scans	8	8
Number of observed targets	1834	1873
Number of observed tilt angles	16	16
Number of object points	236	240
Number of additional parameters	6	6
Total number of unknowns	762	774
Number of datum constraints	4	4
Total number of observations	5518	5635
Degrees-of-freedom	4760	4865

Table 2. RMS of residuals (v) of the spherical observations from the adjustments with and without the inclusion of additional parameters.

	No APs	With APs added	% improvement
Dataset 1			
RMS v_ρ (mm)	0.3	0.3	0
RMS v_θ (")	13.8	9.8	41
RMS v_α (")	16.2	10.5	54
Dataset 2			
RMS v_ρ (mm)	0.3	0.3	0
RMS v_θ (")	15.7	10.8	45
RMS v_α (")	18.3	9.8	87

The additional parameters and their estimated standard deviations are presented in Table 3. In most cases the APs are small, sub-millimetre in the case of the rangefinder offset, a_0 , and less than 10" for the angular coefficients except the vertical circle index error, c_0 , which is several times larger. All, however, are statistically significant at the 95% confidence level. No high correlation coefficients exist among the APs or between the APs and the exterior orientation parameters. The largest coefficient observed was 0.29 between a_0 and the scanner position elements (X_O and Y_O).

Table 3. Estimated additional parameters, standard deviations and significance measures (estimate / standard deviation)

	AP estimate	AP σ	Significance measure
Dataset 1			
a_0 (mm)	0.6	0.02	30.45
b_1 (")	-4.2	0.3	15.20
b_2 (")	4.3	0.7	5.77
b_3 (")	6.1	0.4	16.78
b_4 (")	-2.6	0.4	6.80
c_0 (")	-25.7	0.5	53.65
Dataset 2			
a_0 (mm)	0.6	0.02	31.27
b_1 (")	-4.0	0.3	14.88
b_2 (")	8.1	0.7	10.92
b_3 (")	3.0	0.4	8.39
b_4 (")	-1.0	0.4	2.62
c_0 (")	-33.9	0.5	71.42

Examples from the model identification process are shown in Figures 3 and 4. In each case a clear systematic trend can be seen in the corresponding adjustment residuals. In Figure 3a), the trend is the expected 180° period sinusoidal error resulting from a vertical circle index error (Lichti et al., 2011). Similarly, the sinusoidal trend due to non-orthogonality between the vertical axis and the plane containing the horizontal encoder can be seen. Addition of the corresponding error models (Equation 2) results in self-calibration residuals free from the systematic trends.

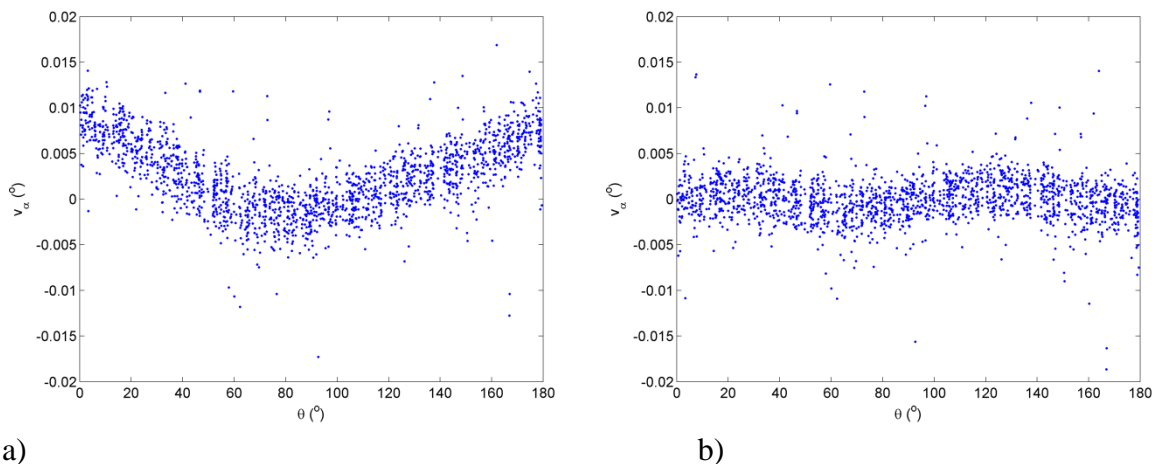
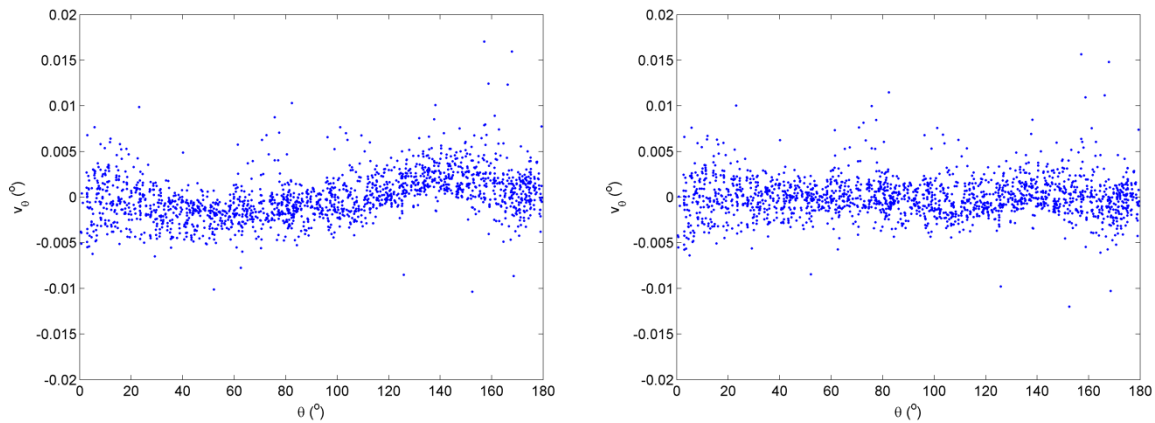


Figure 3. Elevation angle residuals as a function of horizontal direction: a) without vertical circle index error model; b) with model.



a) b)
 Figure 4. Horizontal direction residuals as a function of horizontal direction: a) without vertical axis-horizontal encoder non-orthogonality model; b) with model.

5. CONCLUSIONS

The Leica HDS7000 phase-based terrestrial laser scanner was independently calibrated twice using the point-based self-calibration method. The results show that the scanner has a significant systematic distortion in the collimation axis, trunnion axis; vertical axis-horizontal encoder non-orthogonality and vertical circle index. Also a small (0.6 mm) rangefinder offset parameter was estimated. The exact causes of these errors are unknown, but they can be empirically observed in the residual plots repeatedly. The additional parameters chosen for both calibrations successfully reduced systematic trends perceived in the residual plots and improved the distance, horizontal angle, and vertical angle measurement precision. The improvements gained as a result of the modelling were 41% and 45% in the horizontal angle direction residuals and 54% and 87% in the elevation angle residuals for the first and second datasets, respectively

REFERENCES

- Amiri Parian, J., & Grün, A. (2005). Integrated laser scanner and intensity image calibration and accuracy assessment. *The International Archives of the Photogrammetry, Remote Sensing and Spatial Information Sciences* 36 (Part3/W19), 18-23.
- Böhler, W., Bordas Vicent, M., & Marbs, A. (2003). Investigating laser scanner accuracy. *The International Archives of the Photogrammetry, Remote Sensing and Spatial Information Sciences* 34 (Part5/C15), 696-701.
- Chan, T.O., D.D. Lichti and D Belton (2015). A Rigorous Cylinder-based Self-Calibration Approach for Terrestrial Laser Scanners. *ISPRS Journal of Photogrammetry and Remote Sensing*. 99, 84-99.

Chow, J.C.K, Ebeling, A., & Teskey, B.F. (2010). Low Cost Artificial Planar Target Measurement Techniques for Terrestrial Laser Scanning. FIG Congress 2010: Facing the Challenges - Building the Capacity (On CD-ROM). Sydney, Australia: April 11-16.

Chow, J. Lichti, D.D., Glennie, C. and Hartzell, P. (2013) Improvements to Static Terrestrial LiDAR Self-Calibration. *Sensors*. 13 (6), 7224-7249.

Dorninger, P., Nothegger, C., Pfeifer, N., & Molnár, G. (2008). On-the-job detection and correction of systematic cyclic distance measurement errors of terrestrial laser scanners. *Journal of Applied Geodesy* 2 (4), 191-204.

García-San-Miguel, D., and J.L. Lerma (2014). Geometric calibration of a terrestrial laser scanner with local additional parameters: An automatic strategy. *ISPRS Journal of Photogrammetry and Remote Sensing*. 79, 122-136.

Gielsdorf, F., Rietdorf, A., & Gruendig, L. (2004). A concept for the calibration of terrestrial laser scanners. In: *Proceedings FIG Working Week (on CD-ROM)*. Athens, Greece: International Federation of Surveyors.

Holst, C. and H. Kuhlmann (2014) Aiming at self-calibration of terrestrial laser scanners using only one single object and one single scan. *Journal of Applied Geodesy*. 8 (4), 295-310.

Kersten, T., Sternberg, H., Mechelke, K., & Acevedo Pardo, C.(2005). Investigations into the Accuracy Behaviour of the Terrestrial Laser Scanning System Mensi GS100. *Optical 3-D Measurement Techniques VII*, Gruen & Kahmen (Eds.), Vol. I , 122-131.

Kersten, T., Sternberg, H., Mechelke, K., & Acevedo Pardo, C. (2004). Terrestrial laser scanning system Mensi GS100/GS200 - Accuracy tests, experiences and projects at the Hamburg University of Applied Sciences. *ISPRS*, Vol. XXXIV, Part 5/W16, www.tu-dresden.de/fghfipf/photo/PanoramicPhotogrammetryWorkshop2004/Proceedings.htm .

Lichti, D.D. (2007) Modelling, calibration and analysis of an AM-CW terrestrial laser scanner. *ISPRS Journal of Photogrammetry and Remote Sensing*. 61 (5), 307-324.

Lichti, D., Stewart, M., Tsakiri, M., & Snow, A. (2000). Calibration and testing of a terrestrial laser scanner. *The International Archives of the Photogrammetry, Remote Sensing and Spatial Information Sciences* 33 (part B5/2), 485-492.

Lichti, D., Gordon, S., Stewart, M., Franke, J., & Tsakiri, M. (2002). Comparison of digital photogrammetry and laser scanning. *CIPA WG 6 International Workshop on Scanning Cultural Heritage Recording* (pp. 39-44). Corfu, Greece: 1-2 September 2002.

Lichti, D., Brustle, S., & Franke, J. (2007). Self-calibration and analysis of the Surphaser 25HS 3D scanner. *Strategic Integration of Surveying Services, FIG Working Week 2007* (p. 13). Hong Kong SAR, China: May 13-17, 2007.

Self-Calibration of a Leica HDS7000 Scanner (7889)
Khalil Al-Manasir (China, PR) and Derek Lichti (Canada)

Lichti, D.D., J. Chow, and H. Lahamy (2011). Parameter de-correlation and model-identification in hybrid-style terrestrial laser scanner self-calibration. *ISPRS Journal of Photogrammetry and Remote Sensing*, 66 (3), 317-326.

Molnár, G., Pfeifer, N., Ressel, C., & Dorninger, P. N. (2009). Range calibration of terrestrial laser scanners with piecewise linear functions. *Photogrammetrie, Fernerkundung, Geoinformation* 1 , 9-21.

Reshetyuk, Y. (2006). Calibration of terrestrial laser scanners callidus 1.1, Leica HDS 3000 and Leica HDS 2500. *Survey Review* 38 (302) , 703-713.

Reshetyuk, Y. (2009). Self-calibration and direct georeferencing in terrestrial laser scanning. Doctoral Thesis. Department of Transport and Economics, Division of Geodesy, Royal Institute of Technology (KTH), Stockholm, Sweden, January .

Rüeger, J. (1990). *Electronic Distance Measurement: An Introduction*, 3rd Ed. Heidelberg, Germany: Springer-Verlag.

Schneider, D., & Schwalbe, E. (2008). Integrated processing of terrestrial laser scanner data and fisheye-camera image data. *The International Archives of the Photogrammetry. Remote Sensing and Spatial Information Sciences* 37 (Part B5) , 1037-1043.

Soudarissanane, S, Lindenbergh, R, Menenti, M, Teunissen, P, 2011. Scanning geometry: Influencing factor on the quality of terrestrial laser scanning points, *ISPRS Journal of Photogrammetry and Remote Sensing*, 66 (4), 389-399.

Wolf, P., & Ghilani, C. (2006). *Elementary Surveying: An Introduction to Geomatics* 11th Ed. New Jersey: Pearson Prentice Hall.

BIOGRAPHICAL NOTES

Dr. Khalil Al-Manasir is currently an assistant professor at the University of Nottingham, Ningbo, China (UNNC) and a member of the Chartered Institution of Civil Engineering Surveyors (ICES). His research interest including research projects in digital photogrammetry, laser scanning and UAS acquisition systems to produce complete, high accurate 3D models for several applications such as Building Information Modelling (BIM), heritage documentation, deformation monitoring and mapping.

Dr. Derek Lichti is currently Professor and Head of the Department of Geomatics Engineering at the University of Calgary, Canada, and Editor-in-Chief of the ISPRS Journal of Photogrammetry and Remote Sensing. His research program is focused on developing solutions for the exploitation of optical and range-imaging sensors for the automated creation of accurate, 3D models for measuring human motion, monitoring structural deformation and compiling asset inventories of the built environment.

CONTACTS

Dr. Khalil Al-MANasir
Department of Civil Engineering
Nottingham University Ningbo
199 Taikang East Road,
Ningbo 315100
CHINA

Tel. +86 (0) 574 8818 3141

Fax +86 (0) 574 8818 0175

Email: khalil.manasir@gmail.com

Web site: <http://www.nottingham.edu.cn/en/science-engineering/staffprofile/dr-khalil-al-manasir.aspx>

Prof. Derek Lichti
Department of Geomatics Engineering
The University of Calgary
2500 University Dr NW
Calgary AB T2N 1N4
CANADA

Tel: +1 403 210 9495

Fax: +1 403 284 1980

Email: ddlichti@ucalgary.ca

Web site: <http://www.ucalgary.ca/lichti/>

Self-Calibration of a Leica HDS7000 Scanner (7889)
Khalil Al-Manasir (China, PR) and Derek Lichti (Canada)

FIG Working Week 2015
From the Wisdom of the Ages to the Challenges of the Modern World
Sofia, Bulgaria, 17-21 May 2015